

# Influence of Post-treatment on the Tribo-mechanical properties of Cermet Coatings

R. Ahmed, S. Stewart, V. Stoica, Heriot-Watt University, UK and T. Itsukaichi, Fujimi Inc., Japan

Whilst innovative advancements in thermal spray technology, especially in terms of characterization of starting powders, coating processes and optimisation of coating process parameters have resulted in coatings of improved quality, there is an ever increasing demand to push the frontiers of coating applications. Post-treatment of thermal spray coatings either by HIPing (Hot Isostatic Pressing) or vacuum heating can thus offer one such opportunity by presenting a combination of coating and substrate properties not achievable by individual processes. Hence the aim of this study was to investigate the potential of two integrated process technologies of thermal spraying and HIPing. Tribo-mechanical properties of WC-Co coatings deposited by the HVOF process in the as-sprayed and post-treated conditions were thus investigated in this study. Results are discussed in terms of coating microstructure, sliding wear resistance, elastic modulus, hardness, residual strain and rolling contact fatigue resistance. These results indicate that significant improvements in coating performance can be achieved by appropriate design of post-treated components.

## 1 Introduction

Innovative advances in thermal spraying technology have led it to become an integral part of the aerospace, automotive, metal/paper rolling, oil, construction, marine and biomedical industries. The thrust behind the increasing number of applications is the improved microstructure offered by the advanced coating systems such as HVOF (High Velocity Oxy-Fuel), LPPS (Low Pressure Plasma Spraying), and emerging technologies such as the use of hybrid laser systems and High-Density Infrared (HDI) technology. Excellent corrosive, erosive and abrasive wear resistance of these coatings e.g. WC-Co, WC-Co-Cr have resulted in *environmental friendly solutions* to engineering problems, including improved efficiency, longer life, salvaging of worn/undersized/over-machined components to meet dimensional requirements, and replacement of the hazardous chrome plating process for engineering components.

However, microstructural defects within the coating lower their cohesive and adhesive strength leading to fracture and spalling. Fatigue and delamination of these coatings is a major concern, which has limited their use to low stress industrial applications. Post-treatment of thermal spray coatings [1-3], especially by Hot Isostatic Pressing (HIPing) has been shown to *refine* the microstructure e.g. by eliminating porosity/microcracks, beneficial phase transformations and metallurgical bonding, both within the coating microstructure and at the coating substrate interface. Whilst the industrial demands push existing materials to their limits, there is an urgent need to further investigate the improved coating microstructure for enhanced fatigue and delamination resistance. This will benefit both existing and niche industrial applications of thermal spraying in areas including rollers, shafts, drilling tooling, mining equipment, textile guides, dies, paper rolls, pumps, rolling bearings, gears etc., especially in harsh tribological environments e.g. oil, chemical and food processing industry.

Despite the enormous advantages shown by the post-treatment of thermal spray coatings, studies in the

field of post-treated coatings are scarce. Hence the full potential of post-treated thermal spray coatings is yet to be explored. It is therefore the goal of this research to investigate the tribo-mechanical performance and failure modes of post-treated coating for engineering components, and to explore their potential for high stress industrial applications. This paper reports the comparison of results of the as-sprayed and HIPed WC-Co coatings on the basis of coating microstructure, hardness, elastic modulus, sliding wear, contact fatigue, and residual strain investigations.

## 2 Experimental test procedure

### 2.1 Thermal spraying and HIPing post-treatment

A JP-5000 system was used to spray the WC-12%Co powder on 31mm diameter and 8mm thick AISI 440C steel substrate discs. Industrially optimised deposition conditions were used to spray these coatings in two different thicknesses. These coatings were then ground to attain a final thickness of 50 and 400 microns. The HIPing post-treatment was carried for 1hr at constant pressure (150MPa) in argon environment at temperatures of 850°C and 1200°C. These parameters were selected on the basis of ongoing investigations [4]. To further investigate the influence of HIPing pressure, parallel investigations on the vacuum heat treatment at 1200°C were also conducted, and results compared with those of HIPed conditions. As opposed to most of the previous investigations in this field, this investigation reports the results of uncapsulated HIPing, which has enormous economical and also technical incentives for industrial applications.

### 2.2 Investigations of coating microstructure, hardness and elastic modulus

Microstructural investigations were carried out on polished cross-sections using Scanning Electron Microscopy (SEM), EDX and x-ray diffraction (XRD) analysis. Microhardness measurements were carried out under a load of 300gm using a Vickers microhardness test machine on the coating surface

and cross-section. The elastic modulus of all coating systems was determined by micro-indentation, with a Vickers indenter, using the universal hardness-measuring machine. A load of 500mN was applied for twenty seconds and maintained for five seconds. Measurement of the elastic/plastic response of the unloading curve thus enabled the measurement of modulus. Ten measurements were performed on each coating surface. A distance of 100 $\mu$ m between all indentations was ensured to eliminate stress-field effect from nearby indentations. The indentation modulus ( $Y_{HU}$ ) was determined with the help of following relation:

$$Y_{HU} = \left( 5.59 h_{r'} \frac{\Delta h}{\Delta F} (h_{\max}) - 7.81 \cdot 10^{-7} \right)^{-1} [GPa] \quad \text{Eq. 1}$$

where  $h_{r'}$  is the intersection point of the tangent at the load indentation depth curve for the maximum load and  $\Delta h/\Delta F(h_{\max})$  is the reciprocal slope of the tangent to the load indentation depth-curve at the maximum load [mm/N]. Furthermore, the indentation modulus can be correlated to the Young's modulus (E) of the coating using the relation:

$$E = Y_{HU} (1 - \nu^2) \quad \text{Eq. 2}$$

where  $\nu$  is the Poisson's ratio of the coating. Further details of the test method can be seen in Buchmann et. al. [5].

### 2.3 Rolling Contact Fatigue (RCF) tests

A modified four-ball machine shown in figure 1 was used to investigate the RCF performance of the as-sprayed and HIPed thermal spray coatings. This modification enabled the rotation of the planetary balls to correctly model the kinematics of rolling element discs and precisely defined the contact load. In the current set-up, the coated rolling element disc replaced the upper drive ball, which represented the inner race of the rolling element ball bearing. 50 micron thick coated discs were polished to attain a root mean square (RMS) surface roughness of  $0.1 \pm 0.05 \mu\text{m}$ . Planetary balls were commercial grade 12.7 mm diameter 440-C bearing steel, or hot Isostatically pressed silicon nitride ceramic, with a surface roughness of  $0.01 \pm 0.005 \mu\text{m}$ . These two materials were used to conduct RCF tests in conventional steel ball bearing (steel planetary balls) and hybrid ceramic bearing (ceramic planetary balls) configurations. RCF tests were conducted under full film lubrication conditions, at a spindle speed of  $4000 \pm 10 \text{ rpm}$ , and at an ambient temperature of approximately  $25^\circ\text{C}$ . Failure was defined as the increase in vibration amplitude above a pre-set level. A high viscosity lubricant, Vitrea 320, was used as the tests lubricant, which represented full-film Elasto-Hydrodynamic Lubrication (EHL).

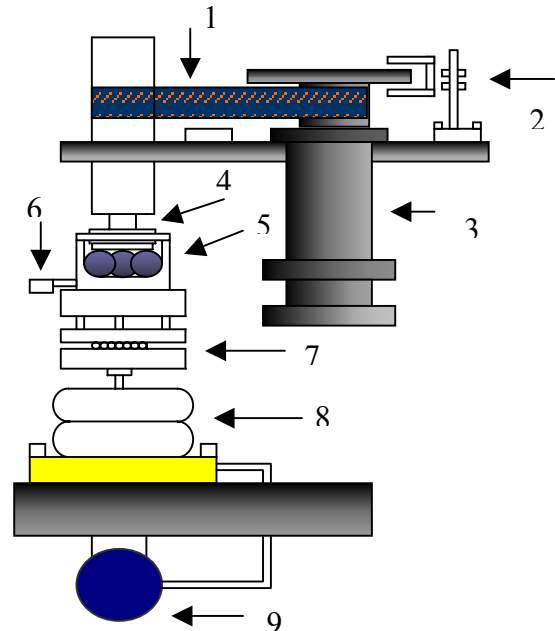


**Fig. 1.** Schematic of modified four-ball machine. (1, Belt drive; 2, Speed sensor; 3, Driving motor; 4, Coated disc and collet; 5, Cup assembly; 6, Thermocouple; 7, Thrust bearing; 8, Bellows; 9, Pressure Gauge).

### 2.4 Sliding wear tests

Sliding wear tests were carried out using a reciprocating ball-on-plate apparatus, instrumented to measure the frictional force via a load cell. In this apparatus the upper ball, bearing the normal load, was stationary while the coated disc had a reciprocating motion. The sliding speed was set as 0.012m/s at the centre of the wear scar. Two types of half inch (12.7mm) diameter balls i.e. AISI 440C bearing steel and silicon-nitride ceramic, were used in this investigation as the counter body, which slid against the 400 micron thick as-sprayed or post-treated coating. The coated specimens were ground and polished to produce a surface roughness ( $R_a$ ) of  $0.04 \mu\text{m}$ . Before each test, the coatings and balls were ultrasonically cleaned in acetone for 5 minutes to remove any contaminants, and then dried in air. Sliding wear tests were performed under two normal loads (12 and 22N) in unlubricated contact conditions at ambient temperature and humidity. The contact stress at the beginning of the tests, corresponding to the loads applied by the steel balls was approximately 180MPa for 12N load and 220MPa for 22N load. When the ceramic balls were used, the contact stress was approximately 210MPa and 255MPa corresponding to the load of 12N and 22N, respectively. Tests at each condition were conducted at least three times and averaged values are reported in next sections. The wear volume was calculated using three dimensional interferometry.

### 2.5 Residual strain Investigations using neutron diffraction

Neutron diffraction analysis was used to conduct residual strain investigations using the Time-Of-Flight (TOF) method [6]. As opposed to conventional x-ray diffraction, this method uses a range of wavelengths of incident beams and the diffraction angle is fixed at

90 degrees. The experimental arrangement comprised of shifting the centre of gravity of the gauge volume from partially submerged conditions (for near

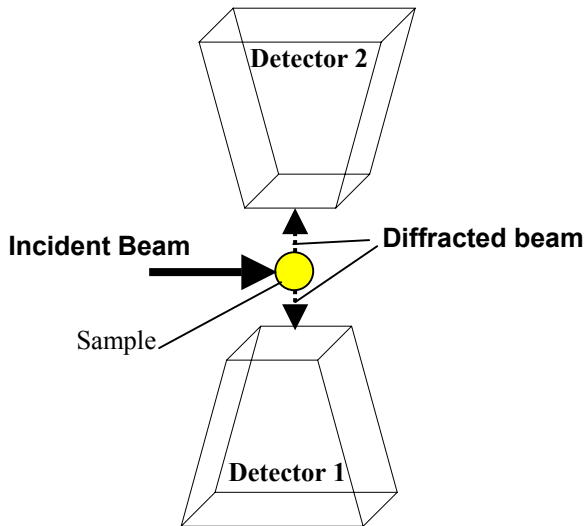


**Fig. 2.** Schematic of neutron diffraction set-up

surface investigations) to fully submerged beams for through thickness analysis. Two detectors, placed at 90 degrees to the incident beam measured the location and intensity of the diffracted beam (figure 2). Residual strain was calculated by considering the shift in the location of the diffracted peaks. Values of stress free lattice parameters ( $d_0$ ) were also calculated using the same method, which was set-up for powder diffraction. The powders for this analysis were produced by detaching the as-sprayed and post-treated coatings from the substrate.

### 3 Results and discussion

#### 3.1 Coating microstructure

Figure 3 shows the SEM comparison of the as-sprayed and HIPed at 1200°C coatings. This figure provides the high magnification microstructural comparison of the as-sprayed and HIPed at 1200°C coatings, whereas the remaining SEM in this figure shows the diffusion layer near the coating substrate interface. These images indicate that HIPing at 1200°C makes the WC faces very prismatic, which indicates diffusion reactions between the WC cermet and Co matrix. XRD investigations of post-treated coatings indicate the formation of mainly  $\text{Co}_6\text{W}_6\text{C}$  (with some other eta-phases), which further support the possibility of interactions between WC and Co, e.g. using the reaction:

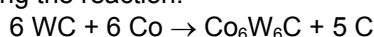


Figure 3 also show a schematic of the summary of events leading to the changes in the coating microstructure observed for the higher temperature (1200°C) post-treatment. The presence of Kirkendall voids, both at the ceramic/cobalt interface within the coating microstructure, and also in the substrate material near the coating substrate interface further

confirmed the diffusion of various elements during the post-treatment. Although not included in this paper, EPMA (Electron Probe Microscopy Analysis) to reveal the elemental dot map of Fe, Cr, W, Co and C in the coating confirmed the diffusion of Fe and Cr from the substrate into the coating, and that of C and Co from the post-treated coating towards the coating substrate interface.

The microstructure of the coatings HIPed at 850°C was similar to the as-sprayed coating. Similarly, coatings vacuum heated at 1200°C were similar to the HIPed at 1200°C, in terms of the changes observed in prismatic WC particles and the diffusion layer. EDX investigation of the diffusion layer indicates W, Fe, Cr, Co. It is not clear at this stage if all of these elements exist in a single crystalline state, and investigations are underway to fully understand the composition of this diffusion layer. As the penetration depth of conventional x-rays in WC-Co material is quite low, without successful removal of the upper layer, XRD investigations of the diffusion layer are impossible. However, the way round the problem was to use neutron diffraction, which has the capability to go through the coating substrate system. To accomplish this, neutron diffraction investigations were made within the coating microstructure, at the coating substrate interface, and in the substrate material by shifting the gauge volume during neutron diffraction analysis. These measurements were made in the as-sprayed and HIPed conditions and a diffraction peak representative of the diffusion layer was identified at an approximate d-spacing of 2.127 Armstrong.

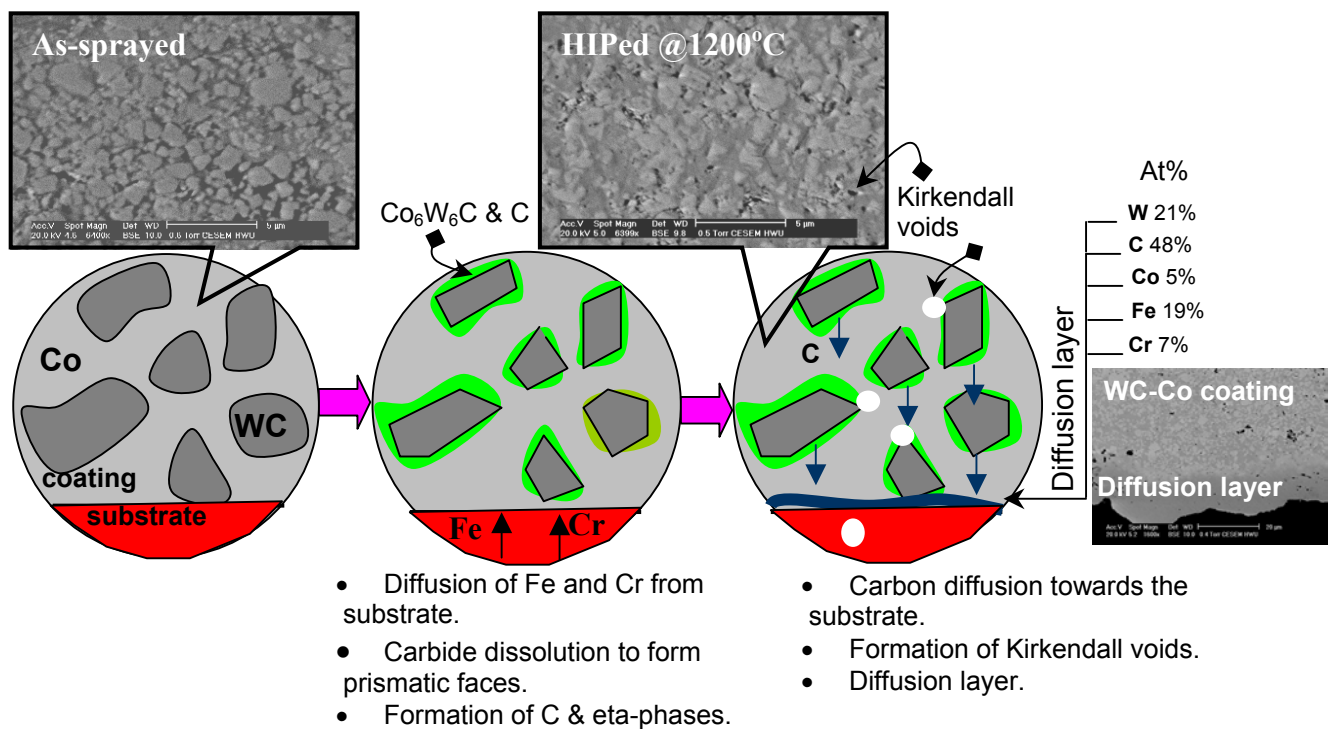
#### 3.2 Microhardness and elastic modulus

Figure 4 shows the variations in coating microhardness in the as-sprayed and post-treated conditions. These results indicate that post-treatment significantly increases the hardness of coating material, which was reflective of the changes seen in the coating microstructure (e.g. eta phases). Figure 5 shows the changes in coating modulus in the as-sprayed and post-treated conditions. This indicates that the bonding mechanism during the post-treatment improved, and metallurgical bonds were formed within the coating microstructure. This is significant as the synergetic increase in hardness and modulus indicates a relatively stronger coating.

#### 3.3 RCF tests

Figure 6 shows the test results obtained from the RCF testing at a contact stress of 2.7 GPa in conventional steel and hybrid ceramic configurations. These results indicate that at higher temperatures of 1200°C, both HIPing and vacuum heating treatments can significantly increase the fatigue performance.

Although the simultaneous increase in hardness and modulus is responsible for this increase in performance, further investigations have confirmed that the formation of diffusion layer (figure 3) near the coating substrate interface was also responsible for this increase in performance. The mechanism of this



**Fig. 3.** Schematic of microstructural changes observed during the post-treatment at 1200°C.

improvement via the diffusion is thought to be the elimination of stress concentrations at the coating substrate interface during the Hertzian loading. The presence of this diffusion layer also resulted in the change in failure mechanism from catastrophic delamination in the as-sprayed coatings, to surface wear in the HIPed at 1200°C coatings. This indicates that for high stress applications, the higher HIPing temperature of 1200°C is better as opposed to 850°C considered in this investigation. As the RCF tests results shown in figure 6, and previous results of coating microstructure, hardness and modulus (figures 4 and 5) do not show significant differences in the HIPed and vacuum heated at 1200°C coatings, the significance of HIPing pressure seems questionable. However, these results do not indicate the severity of RCF failure in the heat treated coatings, as shown in figure 7. Investigation of this difference in the severity of failure for the vacuum heated and HIPed at 1200°C coatings indicated that vacuum heated coatings fail catastrophically, as observed in the as-sprayed coatings, and opposed to the HIPed at 1200°C coatings, indicating the beneficial influence of HIPing over the vacuum heat-treatment.

### 3.4 Sliding Wear Tests

Figure 8 shows the results of sliding wear tests at two different loads of 12N and 22N in contact with both the softer (steel) and harder (ceramic) balls. These results indicate that for the softer counter body (steel ball), post-treatment does not improve the coating's sliding wear resistance, whereas for the harder ceramic counter body, improvements in coating wear resistance is observed, especially for the HIPed at 850°C coatings at both loads. This poses a paradox

when compared to the RCF test results seen in the previous heading, as firstly there are no improvements in coating's wear resistance with steel counter body, and secondly, when the improvements are observed with ceramic counter body, they are more significant with at lower HIPing temperature of 850°C as opposed to 1200°C for the RCF tests. However, this paradox can be resolved by first considering the total wear loss (of both the ball and coating) of the tribological system, and secondly by considering the underpinning wear mechanism.

Figure 9 shows the results of the total volume loss for the steel/coating and ceramic/coating couples. These results indicate that except for the ceramic tests at higher loads, post-treatment of coatings result in improved wear resistance of these test couples. Moreover, coating HIPed at 850°C shows improved performance under all test conditions. These results indicate that for the tests conducted with post-treated coatings, the counter body (steel or ceramic ball) wears less when compared to the as-sprayed couples. But why does the counter body wear less in the case of post-treated coatings? This defies conventional wisdom that the increase in hardness (e.g. in this case the increase in coating hardness after the post-treatment), should theoretically result in higher wear loss of the counter body. Understanding of this behaviour is critical, as it is the total volume loss of the entire system which dictates the tribological performance, and not that of just the coating or counter body, as shown earlier in figure 7.

Examination of worn surfaces indicates that the as-sprayed coating wear track is wider and shallower when compared to the wear track of the post-treated

coatings. It is thought that in the early stages of tests, the wear of the counter body is more significant in the post-treated coatings, as it has higher hardness than

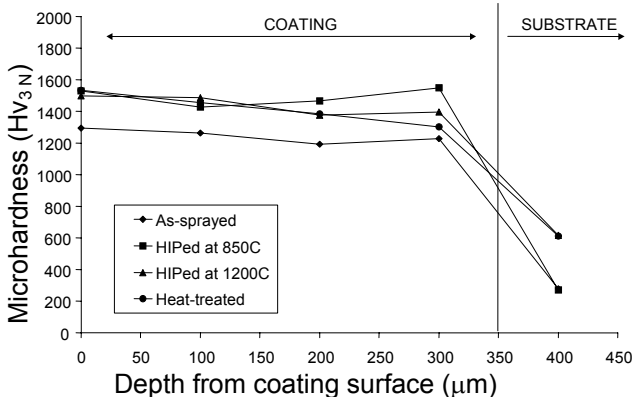


Fig. 4. Microhardness results of the as-sprayed and post-treated coatings.

the as-sprayed coating. The contact area therefore grows faster for the test couple, which comprised of post-treated coatings, in comparison to as-sprayed coatings. Wear debris thus get entrapped in the bigger contact area, and post-treated coatings wear more in the later stages of the test, due to three body abrasion, mainly from hard coating debris. Evidence of this was also observed within the wear scars of post-treated coatings, especially those post-treated at a higher temperature, where abrasive marks were seen along the length of coating wear scar. These debris do not increase the wear loss on the ball, as they embed and roll/slip on the ball surface, but coating wears faster in three body abrasion. Contrary to this, for the as-sprayed tests, there is significantly less three body abrasion, hence coating debris do not entrap and accelerate coating wear. The ball surface therefore loose more material in two body abrasion as the coating wear scar grows wider instead of deeper.

As for the improved wear performance for HIPed at 850°C, it is perceived that this temperature provides the optimum combination of hardness, modulus and coating strength for abrasive resistance. It can be appreciated from figures 4 and 5 that after HIPing at 850°C, the coating attains almost the same hardness and modulus as the HIPed or vacuum heated at 1200°C. However, with the increase in HIPing temperature from 850°C to 1200°C, the extent of both the eta-phases and WC dissolution increases. It is thought that this reduction in WC size results in relatively poor sliding wear performance for coatings post-treated at the higher temperature of 1200°C.

### 3.5 Residual strain

Figure 10 shows the residual strain results of the as-sprayed and HIPed at 1200°C coatings. These results indicate that the HIPed coating has a much more uniform distribution of compressive strain, without any sharp gradient at the coating substrate interface, when compared with the as-sprayed coating. It is appreciated that both of these factors result in

improved coating performance, especially for the high stress RCF tests.

## 4 Conclusions

Microstructural changes associated with the post-treatment of WC-Co coatings can significantly improve tribo-mechanical performance of components. Specific results indicate that:

- 1) RCF performance of coatings improved with the post-treatment temperature, and the best results in terms of performance and failure modes are obtained for coatings HIPed at 1200°C. This improvement was attributed to the diffusion at the coating substrate interface resulting in metallurgical bonding.
- 2) Sliding wear test results indicate that the overall volume loss of the test couples decrease with the post-treatment, and best results were obtained for coatings HIPed at 850°C. This temperature provides the correct balance of inter-lamella bonding (improved modulus), hardness and carbide size.
- 3) Residual stress investigations confirmed that not only the post-treated coatings have lower and more uniform compressive strain, but also the strain gradient at the coating substrate is minimised after the post-treatment.

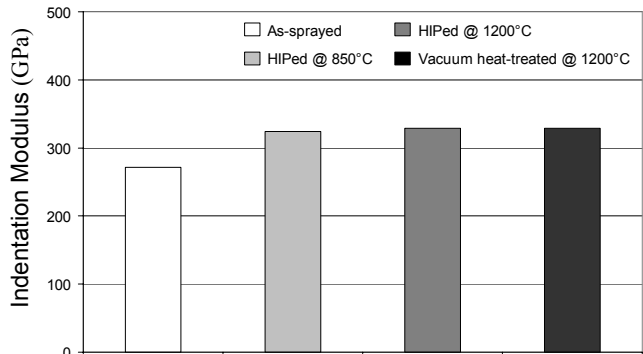


Fig. 5. Changes in coating's modulus after various post-treatments.

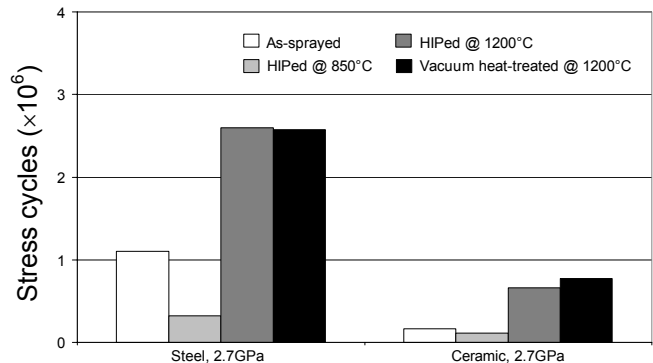
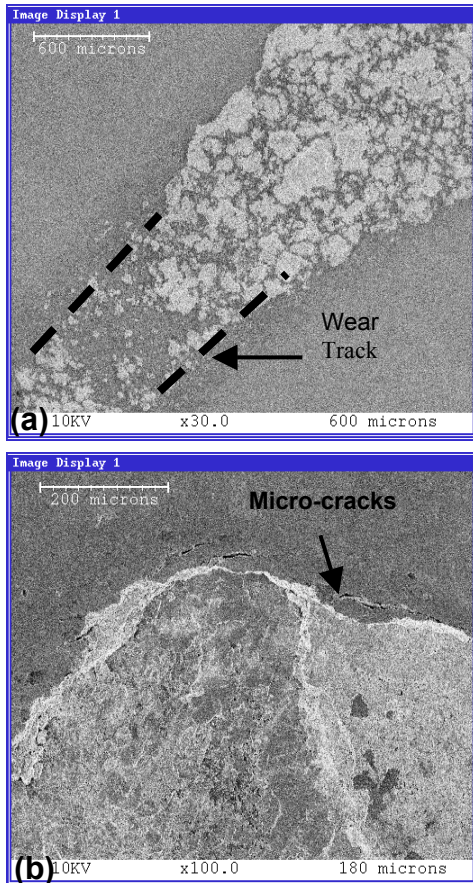
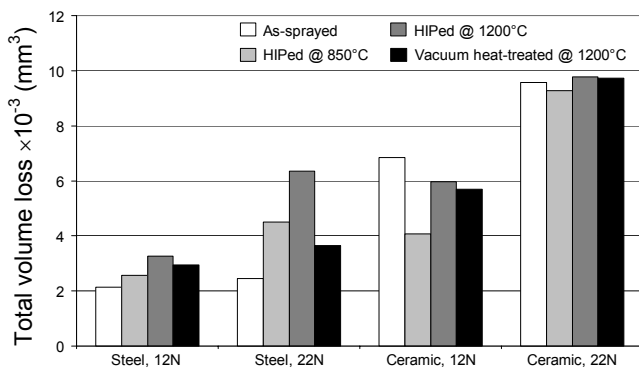


Fig. 6. RCF performance of the as-sprayed and post-treated coatings in steel and hybrid ceramic configurations.



**Fig. 7.** RCF failure of post-treated coatings. (a) HIPed at 1200°C, (b) Vacuum heated at 1200°C



**Fig. 8.** Coating volume loss for various as-sprayed and post-treated test couples.

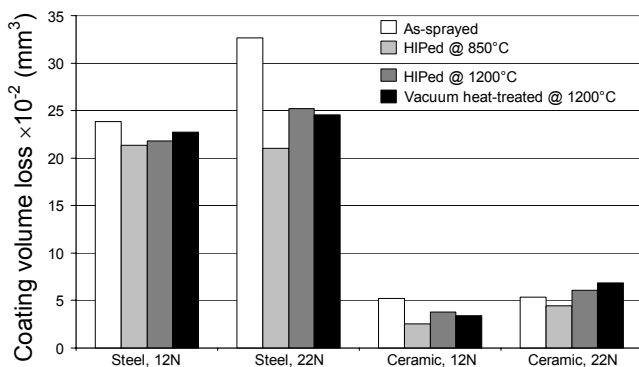


**Fig. 9.** Total (ball and coating) volume loss for various as-sprayed and post-treated test couples.

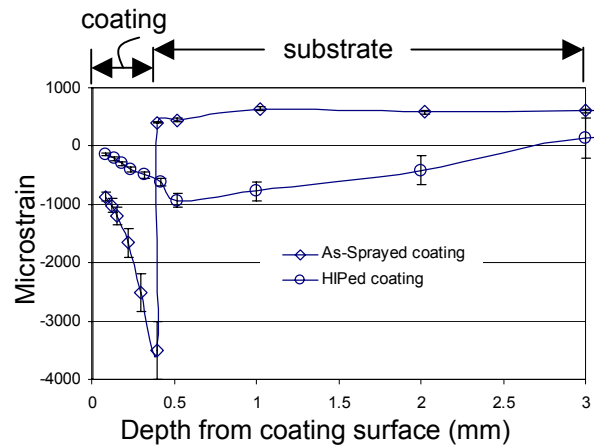


**Fig. 10.** Residual strain measurements in the as-sprayed and HIPed at 1200°C coatings using neutron diffraction.

## 5 References

- [1] Ito, H., Nakamura, R., Shiroyoma, M., & Sasaki, T.: Post-treatment of plasma sprayed WC-Co coatings by hot isostatic pressing. NTSC (1990), CA, pp. 233/38.
- [2] Khor, K.A. & Loh, N. L.: Hot isostatic pressing of plasma sprayed Ni-base alloys. Journal of thermal spraying (1994), 3(1), pp. 57/62.
- [3] Kuribayashi, H., Suganuma, K., Miyamoto, Y., & Koizumi, M.: Effect of HIP treatment on plasma sprayed coating onto stainless steel. American ceramic society bulletin (1986), 65(9), pp. 1306/10.
- [4] Stewart, S., & Ahmed, R.: Contact Fatigue Failure Modes in Hot Isostatically Pressed WC-12%Co Coatings. Surface and Coatings Technology (2003), 172, pp. 204/16.
- [5] Buchmann, M., Escribano, M., Gadov, R., & Burkle, G.: On the elastic mechanical properties of thermally sprayed coatings, Thermal Spray: Surface Engineering via Applied Research, C.C. Berndt, Ed, ASM International (2002), pp. 598/605.
- [6] Santisteban, J.R., Edwards, L. & Fitzpatrick, M.E.: J. Appl. Cryst. 35 (2002), pp.497–504.

## 6 Acknowledgements

The authors would like to thank Dr. Susan Davies at Bodycote Hot Isostatic Pressing Ltd /Infutec Ltd for the HIPing post treatment. Support of Rutherford Appleton Lab, UK (Grant number RB13990) for neutron diffraction analysis is thankfully acknowledged. The authors also acknowledge the financial support of EPSRC, UK (GR / R45284) for their financial contribution in this project.